Funded by the European Union

Sea-ice Surface Temperature Retrieval and Validation for Copernicus Sentinel-3 Sea and Land Surface Temperature Radiometer

Algorithm Theoretical Baseline Document for SLSTR IST algorithms

Document Reference Number: EUM/OPS-COPER/20/1205462

Authors: Gorm Dybkjær and Steinar Eastwood (MET Norway)

Version 1.2

ATBD

Deliverable 7.2 (ATBD v2, D11)

EUMETSAT ITT No. 215580; Contract No. EUM/CO/18/4600002129/AOC

The Danish Meteorological Institute

29-01-2021

Scope of this Report

This report is the final algorithm theoretical baseline document (ATBD v2, D11) for the Copernicus Sentinel-3 Sea and Land Surface Temperature Radiometer (SLSTR) sea-Ice Surface Temperature (IST) prototype processor. The report describes the two implemented sea-ice surface temperature algorithms in detail. The algorithms are evaluated in the Product Validation and Evaluation Report [AD-7].

The work is funded by the European Union under the EUMETSAT Copernicus contract EUM/CO/18/4600002129/AOC

Document Change Record

Version	Date	Author	Description
v1.0	September 16 2020	Gorm Dybkjaer	ATBD v2, D11
v1.1	December 2020	Gorm Dybkjaer	Revised after RIDs
v1.2	January 2021	Gorm Dybkjaer	Revised after extra RIDs

Applicable Documents:

[AD-1] Requirement Baseline Document (RB, D4), Ref. No. EUM/OPS-COPER/19/1065840
[AD-2] Product Validation Plan (PVP, D5), Ref. No. EUM/OPS-COPER/19/1065836
[AD-3] Input Output Data Definition Document (IODD, D6), Ref. No. EUM/OPS-COPER/19/1083003
[AD-4] Product Validation and Evolution Report (PVR, D10)
[AD-5] Project Proposal (internal document available at EUMETSAT)
[AD-6] ATBD Working paper, D7.1 v1.3
[AD-7] Product Validation and Evolution Report (PVR v2, D13), Ref. No. EUM/OPS-COPER/21/1213711

Most AD's are public available at: https://www.eumetsat.int

Table of content

Acronyms and abbreviations

(A)ATSR	(Advanced) Along-Track Scanning Radiometer
ATBD	Algorithm Theoretical Basis Document
AVHRR	Advanced Very High Resolution Radiometer
CAF	Cloud Area Fraction
ECMWF	European Centre for Medium-Range Weather Forecasts
ESA	European Space Agency
EUMETSAT	European Organization for the Exploitation of Meteorological Satellites
GDS	GHRSST Data Specification
GHRSST	The Group for High Resolution Sea Surface Temperature
IST	Sea-Ice Surface Temperature
LST	Land Surface Temperature
Metop	Meteorological Operational (EUMETSAT)
MIZ	Marginal Ice Zone
MIZT	Marginal Ice Zone Temperature
MODIS	Moderate Resolution Imaging Spectroradiometer
NEdT	Noise Equivalent delta Temperature
NWP	Numerical Weather Prediction
OSI SAF	Ocean and Sea Ice Satellite Application Facility
OSI-205	OSI SAF operational L2 IST product based on Metop AVHRR and VIIRS data
QL	Quality Level
RAL	Rutherford Appleton Laboratory
RTM	Radiative Transfer Model
RTTOV	Radiative Transfer for TOVS (TIROS Operational Vertical Sounder)
SLSTR	Sea and Land Surface Temperature Radiometer
SST	Sea Surface Temperature
ST	Surface Temperature
Tb	Brightness Temperature
TCWV	Total Column Water vapour
TIR	Thermal InfraRed
TOA	Top Of Atmosphere
VIIRS	Visible Infrared Imaging Radiometer Suite

1 Introduction

Sea, ice and land surface temperatures are very important for the turbulent and radiative exchange of energy between surface and atmosphere. In sea ice and atmospheric models the surface temperature is an important boundary condition for constraining model state and for model validation. To estimate radiative fluxes within 5 W/m2 of accuracy, the surface temperature must be known to an accuracy of less than 1 K (Stroeve et al., 1996), and optimally without systematic error.

Based on recommendations in the Requirement Baseline Document [AD-1] and in the initial Product Evaluation and Evolution report [AD-4], 2 out of 15tested algorithms are recommended for implementation in the Sentinel-3 SLSTR IST prototype processor. These are the best candidates to comply with the accuracy and precision requirement and performance stability. The two algorithms are 1) a traditional split-window (single view) algorithm and 2) a single-channel/dual-view algorithm. Subsequently, these algorithms are denoted IST2 and IST12, respectively, as a reference to the algorithm naming in the initial PVR [AD-4].

Consequently, the Sentinel-3 SLSTR IST prototype processor provides two parallel IST values in the output file.

2 Product Requirements

There seem to be consensus among IST users and other stakeholders for performance requirements for satellite based IST products of 1 K. This value is often referred to without further specification. In the requirement baseline document [AD-1] it is attempted to trace this requirement to its origin and it turned out that the original 1 K requirement was suggested for a mean area temperature precision, by model communities. In the requirement report and in the validation report [AD-1; AD-7] it is also discussed how performance requirements must be split with regards to in situ observation type due to large variation in observation quality of Arctic in situ measurements.

Based on the Requirement Baseline Document [AD-1] and the experience of the project team within IST retrieval limitations (like failing cloud screening), the precision goal, breakthrough and threshold requirements for SLSTR-IST are set to 1 K, 1.5 K and 2 K. These values are valid for the algorithm accuracy only, i.e. standard deviation of IST error estimates in positively cloud free conditions and against Fiducial Reference Measurements (FRM's). Such conditions are rare and best represented by quality level 5 IST data, evaluated against highest quality in situ observations, e.g. the PROMICE surface temperatures from the Greenland ice cap that are widely used in the validation reports (AD-4 and AD-7).

In order to ensure a state–of-the-art SLSTR IST product, all essential operational state-of-the-art algorithms from IST, LST and SST communities, were tested along with new algorithms with potential improvements in the first validation report [AD-4]. That work led to the choice of 2 algorithms to be implemented for the SLSTR IST prototype processor. The algorithms are described here along with other algorithms applied in the SLSTR IST prototype processor.

3 Satellite Instrument Description

The SLSTR instrument on board Sentinel-3 has nine spectral channels measuring visible, near infrared and thermal infrared wavelengths. These are named in spectral order S1 to S9: the visible channels are S1 around 0.554 microns, S2 around 0.659 microns, and S3 around 0.868 microns; the near infrared or short/ medium wave infrared channels are S4 around 1.374 microns, S5 around 1.613 microns, S6 around 2.25 microns, and S7 around 3.742 microns; the thermal infrared channels are S8 around 10.85 and S9 around 12.02 microns (ESA 2020).

The SLSTR measurement geometry, shown in Figure 1, is showing the overlap between the Nadir and Oblique views. The Sentinel-3 satellite orbits around 815 km with a period around 101 minutes. The SLSTR instrument has two scans for each channel: one across track scan in a nadir/vertical direction, the nadir view, and one rear view scan behind the satellite at an angle of 55 degrees, the oblique view. The nadir view swath width is around 1400 km and the oblique view swath width is around 740 km. The two different views overlap where it is possible to retrieve using both views together, referred to as dual view. The time separation between the two views is about 3 min.

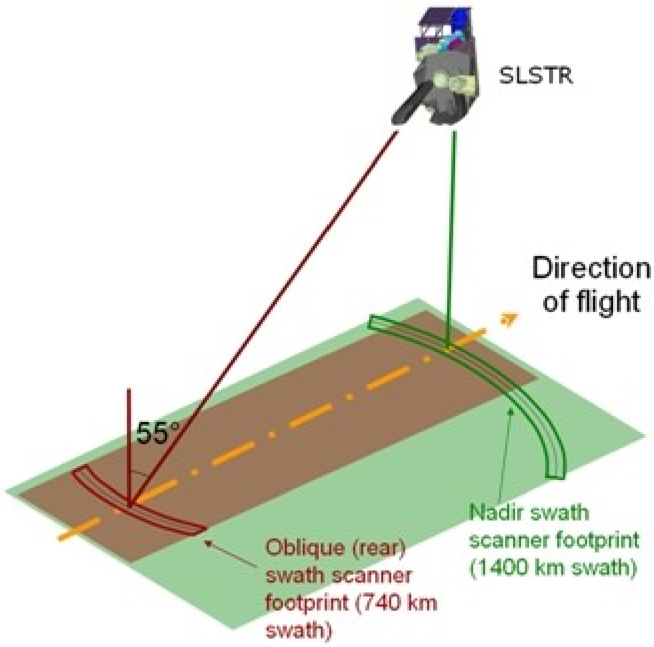

Figure 1 *Sketch of the SLSTR imaging geometry* (*https://sentinel.esa.int/web/sentinel/user-guides/sentinel-3-slstr/coverage*), *showing nadir and oblique views swaths.*

The SLSTR nadir and oblique scans intersect the on-board black bodies and visible calibration unit every other scan providing low-noise high-stability radiometry.

The IST algorithms use the gridded 1 km data (image view) of channels S7, S8 and S9 both from the nadir and oblique view. SLSTR channels are subsequently referred to as $Tb_{\text{<wavelength><view>}}$, for wavelength *11* and *12* microns and view geometry being either *nadir* or *oblique*.

Selected visible channels, S1-S6, are used for the probabilistic SLSTR Sea Ice cloud screening processor (Liberti et al. 2017).

4 SLSTR IST processor algorithms

Several satellite ice surface temperature products are available, all showing similar performance with a standard deviation compared to in situ data typically around 2-4 K, depending on the validation context (Hoyer et al., 2017). With the SLSTR instrument, we expect to generate a satellite product with improved performance relative to existing satellite ice surface temperature products, due to the advanced design of the SLSTR instrument, and experience from the SLSTR predecessors, ATSR and AATSR (e.g. Corlett et al., 2006). In order to provide the best surface temperature product for users, the IST estimates come with associated quality level and uncertainty estimates as means to filter data for any given purpose.

4.1 IST Algorithms

Fifteen IST algorithms were tested and validated prior to the recommendation of a SLSTR IST algorithm (AD-4). From that exercise, the best two algorithms, IST2 and IST12, under different conditions and in various geographical regions are chosen. IST2 is based on nadir view data only, thus providing IST coverage for the wider nadir swath, whereas IST12 is a dual view algorithm that only provides IST for the narrower oblique view swath that overlaps the nadir swath (see Figure 1). The two algorithms are complementary, enabling full resolution IST coverage from IST2, plus the limited coverage from IST12 to be applied in conditions where dual view is superior to IST2. The revisit time of IST12 is naturally lower than for IST2, due to the narrow swath.

The two selected IST algorithms are referred to as IST2 and IST12, with Tb11 and Tb12 being the input brightness temperatures around 11 and 12 microns, respectively (see Chapter 2). Oblique and nadir refer to the sensor view and $a0$, $a1$, …, ai are calibration coefficients. θ is the scan/view angle.

IST2 is a split-window algorithm where the last term is a correction term for angular dependencies of the atmospheric and surface emissivity spatial variability. The algorithm uses two spectral channels (Tb_{11} and Tb_{12}) and only the nadir view:

$$IST2 = a_0 + a_1 Tb_{11nadir} + a_2 Tb_{12nadir} + a_3\left((Tb_{11nadir} - Tb_{12nadir})\left(\frac{1}{\cos\theta} - 1\right)\right)$$

IST12 is a single-channel/dual-view algorithm (see also section 5.4). This algorithm uses one channel in both views, namely $Tb_{11nadir}$ and $Tb_{11oblique}$:

$$IST12 = a_0 + a_1 Tb_{11nadir} + a_2 Tb_{11oblique}$$

4.2 Marginal Ice Zone Temperature (MIZT)

The SLSTR IST is also defined for the marginal ice zone, MIZ. One central requirement for the IST processor is to ensure a seamless transition from closed ice to open water (AD-1). That implies a well-defined MIZ and that the MIZ temperature shall couple with both IST and SST in a seamless manner. Here, the MIZ is enclosed by a warm and a cold threshold of the $Tb_{11nadir}$ temperature. Any pixel colder that the cold threshold deploys the IST algorithms and any pixel warmer than the warm threshold deploys the SST algorithm, where the latter is represented by the SLSTR WST SST with quality level (QL) greater than 1. The MIZ is any pixel within the brightness temperature interval of $268.95\ K \leq Tb_{11nadir} < 270.95\ K$. The seamless MIZT is ensured by a linearly scaled temperature between the nearest SST and the pixel IST. This approach is adopted from the EUMETSAT Ocean and Sea-ice Satellite Application Facility (OSI-SAF, osi-saf.eumetsat.int) IST production (Dybkjaer et al., 2018) for Metop AVHRR.

The MIZT is formulated as follows:

$$MIZT = 0.5*(Tb_{11nadir} - 268.95)*SST - 0.5*(Tb_{11nadir} - 270.95)*IST$$

Here *IST* is the SLSTR IST (IST2 or IST12) and SST is the corresponding SLSTR Level 2P WST SST within a distance of 7 pixels. If no WST SST value is found within the spatial limit, then the SST is fixed at 271.35 K, the freezing temperature of water with salinity of 32 psu, i.e. a typical salinity of Arctic Ocean surface water.

The MIZT algorithm is applied over ocean only, which is the area of application of current processor. However, as a test product the SLSTR IST processor does also cover the two great ice sheets on Antarctica and Greenland. On the ice sheets IST2 and IST12 are applied for all temperatures.

The dependence on the WST SST should be noted for any operational implementation (see also Chapter 8).

4.3 Performance estimates and validation

Performance evaluation of algorithms in the SLSTR IST prototype processor is based on 1 year of match-up data, as specified in the Product Validation Plan [AD-2]. The validation results are presented in details in the Product Validation Report [AD-7].

Monthly mean algorithm performance numbers for IST2 and IST12 are shown in Figure 2, for the 3 sun elevation regimes day time, night time and twilight.

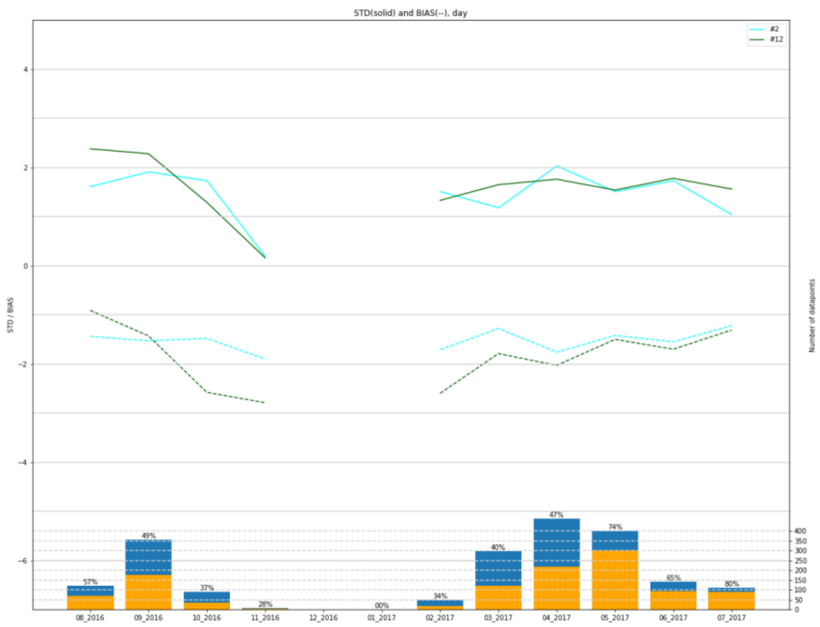

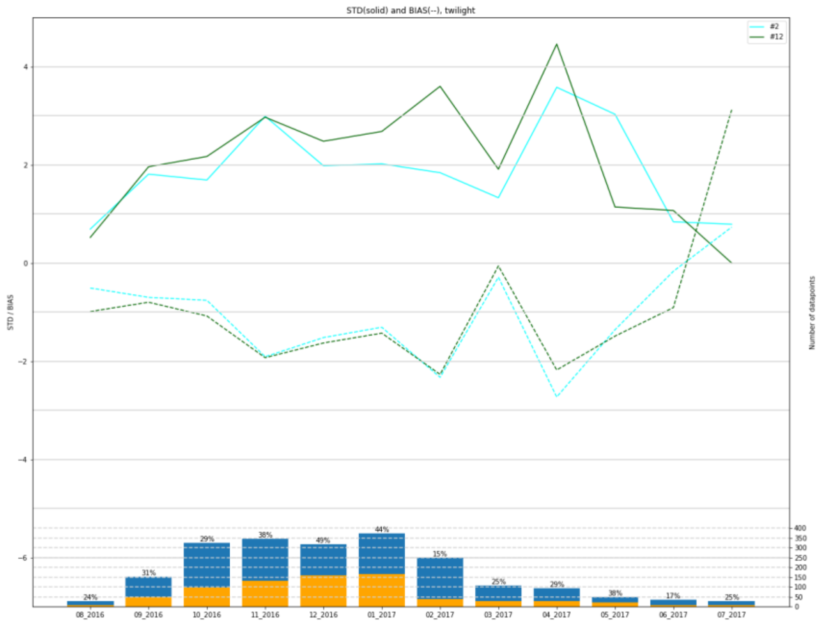

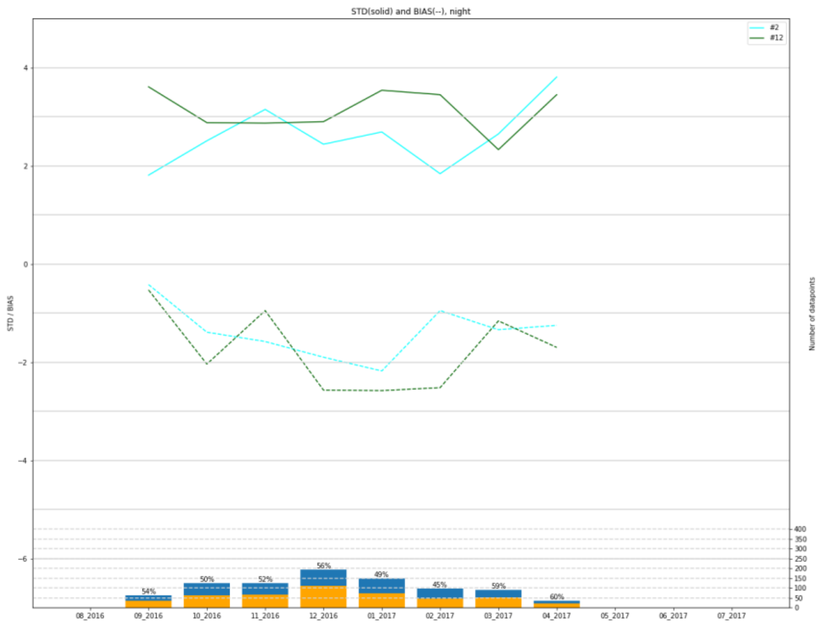

Figure 2 *Quality levels 4 and 5 performance of IST 2 and IST12 (STD in solid lines and Bias in punctured lines). Day time (top panel), twilight (middle panel) and night time (bottom panel). Bars indicate the number of data points before and after masking for IST2 (blue and yellow, respectively). Percentage data remaining after cloud masking is written on the top of the bars. The corresponding statistics for cloud screening for IST12 is similar to the IST2 statistics.*

The validation statistics reveal that the daytime algorithms perform at or better than the given threshold performance of 2 K, except for IST 12 in January and February, where performance is slightly above threshold accuracy. The two algorithms perform equally well over the year, but with shifting "best algorithm" from month to month.

In the Validation report [AD-7] it is argued that both algorithms are expected to perform well under threshold accuracy and that the performance values shown in Figure 2, is worsened by limitations of the applied cloud screening means and to some extent also worsened by observation inaccuracy.

5 Generation of IST retrieval coefficients

The SLSTR IST retrieval coefficients are calculated using regression analysis on RTTOV 12.3 (Hocking et al. 2019) simulations. The setup for these calculations is as follows:

1. Selection of ECMWF atmospheric profiles.
2. Simulation of surface emissivity values for sea ice.
3. Simulating SLSTR brightness temperatures (BT) with RTTOV.
4. Calculating IST algorithm coefficients by regression analysis.

5.1 Selection of ECMWF atmospheric profiles

ECMWF atmospheric profiles are selected separately for the Northern and Southern Hemispheres, using the air temperature and humidity for the surface and pressure levels from ERA Interim reanalysis (Dee et al., 2011), at times 00, 06, 12 and 18 UTC. Only profiles from assumed cloud free conditions are selected by using a threshold applied to the model total cloud cover of < 5%. Profiles over sea ice are identified by selecting those where the model sea ice concentration is > 95%, and surface temperature less than 272K. To have a reasonable large set of simulated radiances for the regression analysis, representative for all seasons are applied. Profiles from 2011 were used, and data thinning was applied by only selecting every 5th latitude and longitude and every 5th day. In total 35360 profiles were used. These are the same profiles that was used for the OSI SAF IST algorithm development (Dybkjaer et al. 2018). The locations for the profiles from the Northern Hemisphere are shown in Figure 3.

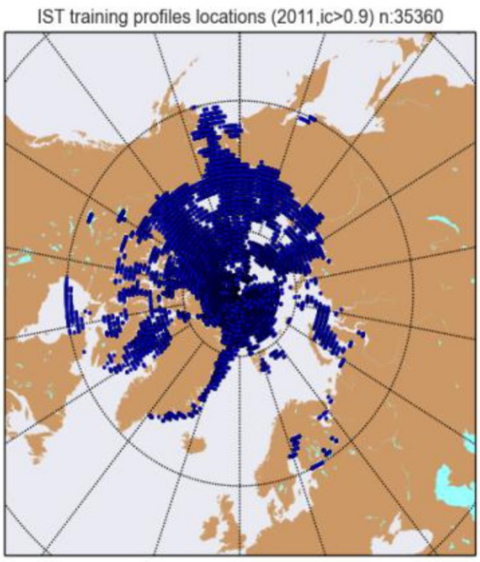

Figure 3 *Location of profiles used for simulation of brightness temperatures.*

5.2 Simulation of surface emissivity values for sea ice

Surface emissivity values are needed for simulating surface brightness temperatures. For IST algorithms over sea ice it is assumed that the sea ice is snow covered, and an updated version of the surface emissivity model by Dozier and Warren (1982) is used to calculate the emissivity as a function of incidence angle for snow with gain size radius of 100 microns for the two applied SLSTR IR channels (10.8 μm and 12.0 μm) integrating over the prelaunch spectral response function for each channel. The algorithm is therefore best calibrated for sea ice with snow on top, which represents most part of the year, except when the sea ice is newly formed, and when it melts and refreezes Emissivity changes for wet snow can give uncertainties of several K on the IST estimate. This is not investigated further here.

5.3 Simulating SLSTR brightness temperatures (Tb) with RTTOV

For simulating the SLSTR IR channels brightness temperatures, RTTOV version 12.3 was used. RTTOV was run without solar radiation, without cloud simulations, using RTTOV interpolator, using Chou-scaling for thermal emitted radiation and using 8 DOM streams. For each atmospheric profile with its surface and 49 pressure levels with air temperature, humidity and pressure, the three SLSTR IR channel Tb values are simulated for 6 satellite zenith angles; 0, 33.5, 44.3, 51.3, 55.0 and 60.0 degrees. These angles represent the range of satellite zenith angles for the nadir view channels, considering that the atmospheric path length is a function of 1/cos(satellite-zenith angle). The 55.0 degree angle is use to simulate the oblique view channels, which have a fixed rotational satellite zenith angle. For dual view algorithms the nadir satellite angles 0 and 33.5 represent the range of angles needed, as the overlapping area between oblique view and nadir view is about 6 to 34 degrees. The nadir view minimum angle is 6 degrees, however, the simulations range from 0 degree view angle.

5.4 Calculating IST algorithm coefficients by regression analysis

The simulated brightness temperatures are used in a multiple regression analysis to calculate the IST algorithm coefficients. For IST2, which uses only nadir view channels, simulated brightness temperatures from all satellite zenith angle were used, thus providing an algorithm that is calibrated for the full range of possible viewing angles.

The dual view algorithm, IST12, uses a combination of oblique and nadir viewing channels. The simulated brightness temperatures for 55 degrees were used for the oblique view channel in combination with brightness temperatures from view angles of 0 and 33.5 degrees for the nadir view channel.

This procedure enables IST12 to encompass all nadir view angles without including a view angle correction term, at the expense of a slightly higher algorithm uncertainty (see STD of fit in Table 1 and Table 2). The regression uncertainty of an alternative IST12 algorithm (IST12 + a view angle correction term) was approximately 0.1 K lower than those of IST12 (not shown), but the performance of the angle corrected IST12 performed consistently worse than or equal to IST12 (AD-4).

5.5 Algorithm coefficients

From the procedure above, the derived coefficients for IST2 and IST12 and the corresponding regression standard deviation for the Northern and the Southern Hemisphere are given in Table 1 and Table 2.

Table 1 *The coefficients and regression fit for SLSTR-S3A and S3B in the Northern Hemisphere.*

NH	a0	a1	a2	a3	Uncertainty of fit (U_{fmt}, STD) [K]
S3A Eq. 2	-0.6384	2.444	-1.442	-0.0633	0.072
S3A Eq. 12	-0.3952	2.3205	-1.3193	-	0.137
S3B Eq. 2	-0.7393	2.4127	-1.4096	-0.0594	0.072
S3B Eq. 12	-0.4190	2.3235	-1.3222	-	0.136

Table 2 *The coefficients and regression fit for SLSTR-S3A and S3B in the Southern Hemisphere.*

SH	a0	a1	a2	a3	Uncertainty of fit (U_{fmt}, STD) [K]
S3A Eq. 2	-1.8837	2.1576	-1.1497	0.1658	0.055
S3A Eq. 12	-3.0656	1.5007	-0.4880	-	0.126
S3B Eq. 2	-1.9800	2.1507	-1.1425	0.1493	0.055
S3B Eq. 12	-3.0917	1.5178	-0.5050	-	0.126

6 Ice surface temperature uncertainty algorithm

For each pixel with a surface temperature estimate, the random, local systematic and large-scale systematic uncertainty is estimated. These uncertainty components represent errors that have discrete correlation properties. The components of the applied uncertainty algorithm for the SLSTR IST product are described in this section. The algorithm is conceptually identical with the OSI SAF IST uncertainty algorithm (Dybkjaer et al., 2018). The specific differences from the OSI SAF IST are inclusion of dynamically pixel-wise NEdT values as opposed to constant sensor values; Global uncertainties and residual of fit are specific for SLSTR.

6.1 The geolocation and instrument noise random uncertainties

The random uncertainty, U_{rnd}, is caused by errors that are unlikely to be correlated spatially. It is split into two components: 1) geolocation precision uncertainty (U_{geo}) and 2) the noise equivalent differential temperature (U_{NEdT}). These two components are combined to make up the random component in the uncertainty budget:

$$U_{rnd} = \sqrt{U_{geo}^2 + U_{NEdT}^2}$$

The uncertainty due to satellite geolocation inaccuracy in mixed pixels with both ice and water is found using the following equation, taking into account the expected geolocation accuracy, the temperature difference between ice and water, and the sea ice concentration:

$$U_{geo} = \left| T_{freeze} - \left(T_{ice} - T_{freeze} * \left(1 - N_{ice} \right) \right) / N_{ice} \right| * C_{geo}$$

where N_{ice} is the sea ice concentration, T_{ice} is the temperature of the sea-ice surface in Kelvin, T_{freeze} is the freezing temperature of sea water (271.35K) and C_{geo} is a geolocation coefficient. The geolocation coefficient is an empirical factor, which is estimated using a satellite imaging resampler. It estimates the temperature uncertainty by shifting a 1 km SLSTR pixel by the geolocation uncertainty under different ice concentrations conditions (DMI 2020). Its magnitude depends on the geolocation accuracy and the footprint size. In cases where the ice concentration is below 15 % or above 85 % U_{geo} is set to zero because of the limited inter pixel SST/IST variability over open water and closed ice. The upper limit of U_{geo} is constrained to 2 K.

Tests with a satellite imaging simulator/resampler shows that C_{geo} is approximately linear at sub-pixel resolution and it can be scaled to fit other satellites with comparable footprint size by taking into account their geolocation precision. As an example, assuming the pixel size of the SLSTR instrument is approximately equal to that of the VIIRS instrument (1000 m vs. 750 m) while their geolocation accuracies are 1000 m and 100 m respectively (values provided by operators), the geolocation coefficient for VIIRS is therefore:

Example: C_{geo} (VIIRS) = 100m/1000m * C_{geo} (AVHRR)

The geolocation coefficient for the SLSTR 1 km grid is similar to Metop AVHRR, which is 0.1 (Dybkjaer et al., 2018)

Noise equivalent differential temperature (NEdT) is radiometer specific and it is expected to depend on e.g. the scene temperature. Values of U_{NEdT} can be determined from propagating perturbed brightness temperature through each algorithm or by estimating it mathematically, as it is done here. Here the NEdT values are calculated by a pixel-wise method developed at RAL space (2019). Code delivered by Gary Corlett, EUMETSAT (2020).

6.2 Uncertainty correlated on local scales

The local scale uncertainty component, U_{loc}, combines the uncertainty introduced by the emissivity variations due to the changes in satellite zenith angle and surface emissivity dependent uncertainty, and the residual of the fit (U_{fmt}) for the regression-based retrieval algorithm:

$$U_{loc} = \sqrt{U_{emis} + U_{fmt}}$$

The uncertainty due to emissivity variability is simulated using a snow emissivity model described in an updated version of the Dozier and Warren (1982) model, using standard snow grain size and density.

The emissivity and its variability is a function of the satellite zenith angle. The uncertainty due to surface snow emissivity, U_{emis}, is therefore given as a function of satellite zenith angle (SatZenAngle):

$$Uemis = 0.0001 * SatZenAngle + 0.0379, \text{ for angles of } 0-44 \text{ degrees}$$
$$Uemis = 0.0030 * SatZenAngle + 0.0912, \text{ for angles of } 45-80 \text{ degrees}$$

The uncertainty component caused by algorithm dependent uncertainty is given as the residual of the fit for the regression used to estimate the algorithm coefficients are found in Table 1 and Table 2.

6.3 Uncertainties correlated on large and global scales

The large-scale/globally correlated uncertainty, U_{glob}, is the global residual uncertainty that is essentially quantified by the data quality levels. The U_{glob} values for each quality level have been set by an expert judgment of the likely magnitude of the residual uncertainties. The expert judgement is based on experience from several calibration/validation activities comparing in situ temperature measurements to satellite derived ice surface temperatures. Those activities include comparison of satellite ice surface temperature measurements against multiple ground based radiometer data sets, air temperature data sets and data sets from Ice Mass-balance Buoy data sets, e.g. Dybkjaer et al. (2012).

The U_{glob} values used for both IST2 and IST12 are shown in Table 3.

Table 3 *Global scale uncertainties for the different quality levels*

Quality level	Uglob [K]
5	0
4	0.25
3	0.5
2	1
1	2
0	fill value

The total IST uncertainty (U_{tot}) for a single pixel is given as:

$$U_{tot} = \sqrt{{U_{rnd}}^2 + {U_{loc}}^2 + {U_{glob}}^2}$$

and U_{tot} is included in the output file.

7 Data quality levels

Quality levels provide an easy means for users to filter data according to their respective requirements (see AD-7). The quality level is also an input to the uncertainty algorithm, determining the magnitude of the globally correlated component. The GHRSST (GDS v2) specification is adopted for the SLSTR IST product, resulting in six quality levels, QL0-QL5 (see Table 4).

Quality level stratification is based on the degree of compliance to various conditions known to deteriorate the quality of the IST estimate from a statistical point of view. A total of six tests are performed, each raising penalties if the test fails. The sum of penalties (failed tests) determines the QL for any given IST estimate. The six tests are listed in Table 5 including the threshold values and penalty for not complying with test.

Sensor Specific Error Statistic (SSES), STD and Bias, are not determined for each quality level. The fields are included in the output product, but they are empty. It was decided to leave these fields empty; because of limited high quality validation data for sea ice (see AD-7). This work is recommended revisited before operationalization of the product.

Table 4 *Description of 6 point Quality level scale, including the number of penalties that a given QL represents.*

Quality Level	Description	Penalty points
QL 0	No Data. Missing or corrupt data	--
QL 1	Bad Data. Not cloud free according to cloud mask	> 5
QL 2	Worst Quality	4 - 5
QL 3	Low Quality	3
QL 4	Acceptable Quality	1 - 2
QL 5	Best Quality	0

Table 5 *The IST test procedure, where a failed test invokes a penalty*

Test Name	Description	Penalty for failed test
IST	The IST estimate is within 10 K of the corresponding NWP surface temperature value.	1
Sat-Zenith	The scan angle is less than 55 degrees	1
Sun-Zenith	The sun elevation is less than 80 degrees	1
*Cloud	The pixel is cloud free. Test against the nadir sensor cloud product for IST2 and test against both nadir and oblique sensor cloud product for IST12	6
CAF	The NWP cloud area fraction is less than 0.8	1
TCWV	The total column water vapour is less than 3 kg m^{-2} according the associated NWP TCWV	1

* Cloud screening is performed by the composite algorithm, using the binary Basic cloud mask for sun elevations lower that 80 degrees and Liberti cloud mask (cloud if probability-of-cloud > 50%) for sun elevation higher than or equal 80 degrees. The Nadir-view-only IST algorithm, #2, uses Basic-nadir and Liberti-nadir cloud masks and the dual view IST algorithm, #12, uses both Basic-nadir and Liberti-nadir and Basic-oblique and Liberti-oblique cloud masks, i.e. data from #12 are considered cloud contaminated if either of the nadir or oblique cloud masks are set.

8 Practical considerations

The SLSTR IST prototype processor produces Sea-Ice Surface Temperature based on level 1 thermal radiation data, cloud information and level 2 WST SST data, as described in the IODD [AD-3].

The applied SST data is the WST level 2 product corresponding to the given SLSTR IST segment. Consequently, the WST production must run prior to the SLSTR IST prototype processor. In a future operational setup, the SLSTR SST and the IST processors should be integrated, in order for both products to be available in due time for NRT users. However, following present procedure will only extent timeliness by a few minutes, depending on the hardware.

Whether the WST SST product is the best suited SST product for high latitude has not been investigated. Tuning of SST algorithms for the special atmospheric conditions at high latitudes is done for the OSISAF SST products, which did improved performance compared to mid and low-latitude SST algorithms. Tuning of WST products can be considered for future SST WST updates.

Product quality assessment and diagnostics is carried out and presented in the final Validation Report (AD-7), in accordance with the Product Validation Plan (AD-2). The validation procedures from the validation report can to a large extent can be transferred to future routine validations, with error and bias relative to in situ observations as basic metrics. However, it is important to identify in situ data sources of appropriate quality that at the same time can provide the right amount of observations that enables for regular (e.g. half-yearly) and stratified validations, i.e. observations that are spatially and temporally distributed. In the associated validation report (AD-7) issues regarding in situ ice temperature observation quality is being elaborated and suggestions for future in situ temperature monitoring are provided.

Missing data, data failure and other unforeseen and non-realistic outputs are captured by various checks for data availability and data sanity. Erroneous data are replaced by fill values in the output data stream and subsequently given the quality level 0.

The prototype processor is built in Python 3 using standard modules in order to be applicable in all hardware environments without licence limitation and in order to ensure easy transfer of code responsibilities. The software is described in the readme instructions in the installation package on the EUMETSAT GitLab.

Operation of the SLSTR IST processor should be limited to SLSTR segments within the area of interest, i.e. pole-wards of latitudes 50 N and 50 S. A simple processing decision rule can be to process segments with more than 1 pixel inside the area of interest. This will reduce segments of interest with approximately 50 %.

9 Conclusion

A SLSTR IST prototype processor is developed based on experience with existing IST processors and new developments. This document describes all processes and algorithms implemented in the processor, as well as decisions and assumptions made. All settings and calibration coefficients are specified. By combining this document with the IODD [AD-4], it is possible to replicate the prototype processor.

The performance of the new SLSTR IST product has proven comparable or superior to existing IST processors [AD-7]. However, the work has been carried out within a limited timeframe and with limited amount of validation data, so parts of the processor are advised to be revisited for potential improvements.

Some assumptions have been drawn without scientific evidence. For example, it is assumed that algorithm calibrations are representative on hemispheric scale, i.e. assuming uniform snow/ice emissivity on hemispheric scale. We know from model studies that snow emissivity is depending largely on grain size and density and that snow emissivity changes after charging surface characteristics after the first melt event. The applied algorithms do not take such effects into account.

It is also assumed that the marginal ice zone temperature can be expressed as a linear scaling of temperature between IST and SST values. That has never been verified, because of the lack of proper in situ observation from the marginal ice zone.

The two implemented algorithms (IST2 and IST12) are chosen based on thorough testing and validation of 15 new and existing algorithms. It is believed that the implemented algorithms are among the best possible performing algorithms for IST monitoring with SLSTR and that performance improvements shall focus on other parts of the processor.

There is consensus in surface temperature communities that poor performance of cloud screening algorithms over land and sea ice is the dominating error source for IST products, in particular during night time and twilight. Despite the fact that cloud screening algorithm development is outside the scope of this contract, there is no doubt that research on this field is essential.

Further improvements to the IST product can potentially be found in calibration procedures. For example, it was not investigated whether the algorithm calibration will improve if the used RTTOV setup include liquid water or if higher vertical resolution is applied, or if further time and space stratified calibrations will improve algorithm performance.

Moreover, the definition of ice, marginal ice zone and water is based on brightness temperature thresholds, and subsequently the choice of algorithm depends on the given temperature. It should be investigated whether the choice of algorithm shall be based on other indicators, like an ice concentration product.

Is also recommended to compile an appropriate number of high quality in situ observations in order to populate the QL specific SSES-STD and Bias fields of the output product.

Finally, it is strongly advised to review the performance of quality level assignment and uncertainty estimates. This also requires a large amount of SLSTR IST data to be processed and matched up with large numbers of high quality ground observations.

10 Acknowledgement

The work is funded by the European Union under the EUMETSAT Copernicus contract EUM/CO/18/4600002129/AOC

11 Reference

Corlett, G.K., I.J.Barton, C.J.Donlon, M.C.Edwards, S.A.Good, L.A.Horrocks, D.T.Llewellyn-Jones, C.J.Merchant, P.J.Minnett, T.J.Nightingale, E.J.Noyes, A.G.O'Carroll, J.J.Remedios and I.S.Robinson, R.W.Saunders[d]J.G.Watts. The accuracy of SST retrievals from AATSR: An initial assessment through geophysical validation against in situ radiometers, buoys and other SST data sets. Advances in Space Research, Volume 37, Issue 4, Pages 764-769, 2006.

DMI. Personal communication of non-documented work by Rasmus Tonboe (rtt@dmi.dk). 2020

Dee, D.P., S. M. Uppala A. J. Simmons ++, 2011: The ERA-Interim reanalysis: configuration and performance of the data assimilation system. Quarterly Journal of the Royal Meteorological Society, doi: 10.1002/qj.828.

Dozier, J. and S. G. Warren. Effect of viewing angle on the infrared brightness temperature of snow. Water resources research 18(5), 1424-1434, 1982.

Dybkjær, G., R. Tonboe, and J. L. Høyer: Arctic surface temperatures from Metop AVHRR compared to in situ ocean and land data. Ocean Sci., 8, 959–970, doi: 10.5194/os-8-959-2012.

Dybkjaer, G., S. Eastwood, A. L. Borg, and J. L. Høyer, R. Tonboe. OSI SAF Algorithm theoretical basis document for the OSI SAF High Latitude L2 Sea and Sea Ice Surface Temperature L2 processing chain. SAF/OSI/CDOP/DMI/SCI/MA/223, product OSI-205, Version 1.3, 2018.

ESA. https://sentinel.esa.int/web/sentinel/technical-guides/sentinel-3-slstr/instrument/specifications. 202011.

GHRSST Data Specification. GDS v2.0. https://www.ghrsst.org/about-ghrsst/governance-documents/ 2012.

Hocking, J., P. Rayer, D Rundle, R. Saunders, M. Matricardi, A. Geer, P. Brunel and J. Vidot, 2019: RTTOV v12 User Guide. EUMETSAT NWP SAF.

Liberti, G.L., et al.. Cloud-screening over sea-ice and marginal ice zones: final report.. ITT no: 211424. EUM/OPS-COPER/DOC/17/927901, 2017.

RAL space. Sentinel-3 SLSTR Uncertainties in Level-1 Products Algorithm and Theoretical Basis Document. Doc. No.: SLSTR-RAL-EUM-TN-003, 2019.

Stroeve, J., M. Haefliger, and K. Steffen, 1996: Surface Temperature from ERS-1 ATSR Infrared Thermal Satellite Data in Polar Regions. J. Appl. Meteor., 35, 1231–1239, doi.org/10.1175/1520-0450(1996)035

Warren, S. G., and R. E. Brandt. Optical constants of ice from the ultraviolet to the microwave: A revised compilation, J. Geophys. Res., 113, D14220, doi: 10.1029/2007JD009744, 2008.

Zhang, Z.M., B.K. Tsai and G. Machin (Eds.). Radiometric Temperature Measurements: II. Applications. Academic Press, 18. nov. 2009. Remote Sensing of the earth's surface temperature, Chapter 6 Peter Minnett, 2009b.